FROUDE SIMILITUDE AND SCALE EFFECTS AFFECTING AIR ENTRAINMENT IN HYDRAULIC JUMPS

Hubert Chanson[1] and Frédéric Murzyn[2]
[1]Professor in Civil Engineering, The University of Queensland, Brisbane QLD 4072, Australia, Ph.: (61 7) 3365 4163, Fax: (61 7) 3365 4599, E-mail: h.chanson@uq.edu.au
[2]Lecturer, ESTACA Campus Ouest, Parc Universitaire de Laval - Changé Rue Georges Charpak, BP 76121, 53061 Laval Cedex 9, France

Abstract: A hydraulic jump is the rapid transition from a high-velocity to a low-velocity open channel flow. It is characterized by strong turbulence and air bubble entrainment. Detailed air-water flow properties were measured in hydraulic jumps with partially-developed inflow conditions. The present data set together with the earlier data of Chanson (2006) yielded similar experiments conducted with identical inflow Froude numbers but Reynolds numbers between 24,000 and 98,000. The comparative results showed some drastic scale effects in the smaller hydraulic jumps in terms of void fraction and bubble count rate distributions. The present comparative analysis demonstrated quantitatively that dynamic similarity of two-phase flows in hydraulic jumps cannot be achieved with a Froude similitude. In experimental facilities with Reynolds numbers up to 10^5, some viscous scale effects were observed in terms of the rate of entrained air and air-water interfacial area.
Keywords: Hydraulic jumps, Air bubble entrainment, Physical modelling, Froude similitude, Scale effects.

INTRODUCTION

The hydraulic jump is the rapid transition from a supercritical to a subcritical open channel flow. It is characterized by the interaction of a strong turbulence with a free surface leading to air entrainment with macro-scale vortices and kinetic energy dissipation (Fig. 1). A hydraulic jump is defined by its inflow Froude number $Fr_1 = V_1 / \sqrt{g\,d_1}$ where V_1 is the inflow velocity, d_1 is the inflow depth and g is the gravity acceleration. Fr_1 is always greater than unity. Air bubble entrainment in a hydraulic jump starts for $Fr_1 > 1$ to 1.3 (Chanson 1997, Murzyn et al. 2007). The air entrainment is caused by the strong interaction between turbulence and free surface which generates disturbances of the air-water interface and vortex formation leading to some air entrapment. Void fraction measurements in hydraulic jumps were first conducted by Rajaratnam (1962). Resch and Leutheusser (1972) performed hot-film probe measurements in the bubbly flow region and showed some effects of the upstream flow conditions. Recent developments included Chanson (1995), Mossa and Tolve (1998), Chanson and Brattberg (2000), Murzyn et al. (2005) and Chanson (2007).

In this study, detailed air-water flow measurements were performed in hydraulic jump flows for two inflow Froude numbers (Fr_1 = 5 & 8.5, Re= 38,000 & 62,000). The results were compared with an earlier study (Chanson 2006) performed with identical inflow Froude numbers but different geometric scales. The comparative analysis provides new detailed information on scale effects affecting void fraction and bubble count rate distributions in hydraulic jumps with partially-developed inflow conditions.

DIMENSIONAL ANALYSIS AND SIMILITUDE

Theoretical and numerical studies of air bubble entrainment in hydraulic jumps are difficult because of the large number of relevant equations (Chanson 1997,2007b). Experimental investigations are performed with geometrically similar models based upon a dimensional analysis and dynamic similitude. In the study of the hydraulic jump, the Froude similitude is

commonly used because of theoretical considerations (Bélanger 1829, Henderson 1966). But the turbulent processes in the shear region are dominated by viscous forces (Wood 1991, Chanson 1997).

For a hydraulic jump in a smooth, horizontal, rectangular channel, a simplified dimensional analysis showed that the parameters affecting the air-water flow properties at a position (x, y, z) include : (a) the fluid properties including the air and water densities ρ_{air} and ρ, the air and water dynamic viscosities μ_{air} and μ, the surface tension σ, and the gravity acceleration g, (b) the channel properties including the width W, and, (c) the inflow properties such as the inflow depth d_1, the inflow velocity V_1, a characteristic turbulent velocity u'_1, and the boundary layer thickness δ (Chanson 2006,2007b). In addition, biochemical properties of the water solution must be considered and may have some significant effect. If the local void fraction C is known, the density and viscosity of the air-water mixture may be expressed in terms of the water properties and void fraction only; hence the parameters ρ_{air} and μ_{air} may be ignored. The result may be expressed in dimensionless terms:

$$C, \frac{F d_1}{V_1}, \frac{V}{\sqrt{g d_1}}, \frac{u'}{V_1}, \frac{d_{ab}}{d_1} ... = F_1\left(\frac{x}{d_1}, \frac{y}{d_1} \frac{z}{d_1}, Fr_1, \frac{u_1'}{V_1}, Re, Mo, \frac{x_1}{d_1}, \frac{\delta}{d_1}, \frac{W}{d_1}, ...\right) \quad (1)$$

where F is the bubble count rate, V is the velocity, u' is a characteristic turbulent velocity, d_{ab} is a bubble size, x is the coordinate in the flow direction measured from the upstream gate, y is the vertical coordinate, z is the transverse coordinate measured from the channel centreline, and x_1 is the distance from the upstream gate (Fig. 1).

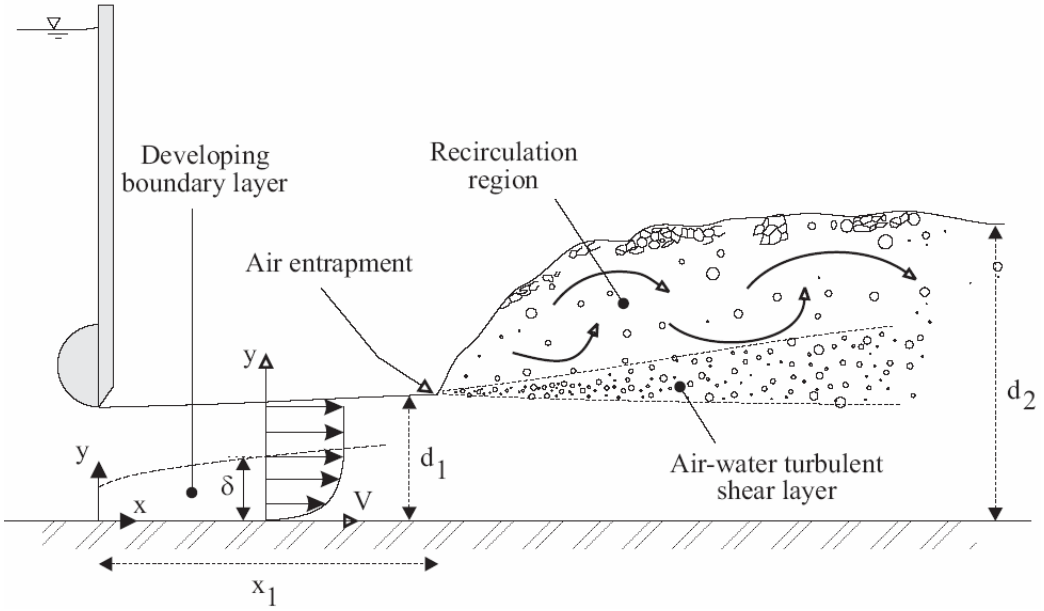

Fig. 1 - Air entrainment in a hydraulic jump with partially-developed inflow

In Equation (1), the dimensionless air-water flow properties at a dimensionless position (x/d_1, y/d_1, z/d_1) within the jump are expressed as functions of the dimensionless inflow properties and channel geometry. In the right handside of Equation (1), the fourth, sixth and seventh terms are the inflow Froude number Fr_1, Reynolds number $Re = \rho V_1 d_1 / \mu$ and Morton number $Mo = g\mu^4 / \rho\sigma^3$ respectively. In Equation (1), the Weber We was replaced

by the Morton number since $Mo = We^3 / (Fr^2 Re^4)$. The Morton number is a function only of fluid properties and gravity constant, and it becomes an invariant if the same fluids (air and water) are used in both model and prototype, as in the present study.

The first systematic study of dynamic similarity and scale effects affecting the two-phase flow properties in hydraulic jumps was the work of Chanson (2006,2007b). For two inflow Froude numbers (Fr_1 = 5.1 & 8.5), the experiments tested the validity of the Froude similitude and the effects of the inflow Reynolds number, with all other relevant parameters being constant :

$$C, \frac{F}{V_1}\frac{d_1}{\sqrt{g\,d_1}}, \frac{V}{V_1}, \frac{u'}{V_1}, \frac{d_{ab}}{d_1} ... = F_2(Re) \qquad \text{Chanson (2007b) (2)}$$

where the Froude number Fr_1 and the relative channel width W/d_1 were constant: i.e., Fr_1 = 5.1 & 8.5, W/d_1 = 20 (Table 1). The results of the Froude-similar experiments showed scale effects in the smaller hydraulic jumps. In the same study, Chanson (2006) tested the effect of the relative width W/d_1, with all other relevant parameters being constant. That is:

$$C, \frac{F}{V_1}\frac{d_1}{\sqrt{g\,d_1}}, \frac{V}{V_1}, \frac{u'}{V_1}, \frac{d_{ab}}{d_1} ... = F_3\left(\frac{W}{d_1}\right) \qquad \text{Chanson (2007b) (3)}$$

where the inflow Froude and Reynolds numbers were constant : Fr_1 = 5.1 & 8.5, Re = 75,000 & 95,000 (Table 1). The results showed that the relative channel width had no effect on the air-water flow properties for :

$$\frac{W}{d_1} \geq 10 \qquad \text{no effect of channel width (4)}$$

In the present study, two experiments were conducted with the same inflow Froude numbers as the study of Chanson (2006) (Table 1). The instrumentation was similar for the present and earlier investigations, including identical sampling rate (20 kHz) and duration (45 s). A systematic comparison between the present and earlier data provide new information on the validity of the Froude similarity to study air bubble entrainment in hydraulic jumps, particularly with reference to the effects of the inflow Reynolds numbers. Note that the present study was conducted with a relative channel width W/d_1 = 28 which satisfied Equation (4).

Table 1 - Physical modelling of two-phase flow properties in hydraulic jumps based upon an undistorted Froude similitude with air and water

Reference	x_1 (m)	d_1 (m)	Fr_1	Re	W/d_1	Instrumentation
Chanson (2006)	1.0	0.024	5.1 8.6	68,000 98,000	20	Single-tip conductivity (∅ = 0.35 mm)
Present study	0.75	0.018	5.1 8.3	38,000 62,000	28	Dual-tip conductivity (∅ = 0.25 mm)
Chanson (2006)	0.5	0.012	5.1 8.4	25,000 38,000	20	Single-tip conductivity (∅ = 0.35 mm)
Chanson (2006)	1.0	0.024	5.0 8.0	77,000 95,000	10	Single-tip conductivity (∅ = 0.35 mm)

Note : Hydraulic jumps with partially-developed inflow conditions

EXPERIMENTAL APPARATUS AND PROCEDURES

New experiments were performed in a horizontal rectangular flume at the Gordon McKay Hydraulics Laboratory of University of Queensland (Fig 2). The channel width was 0.50 m. The sidewall height and flume length were respectively 0.45 m and 3.2 m. The sidewalls were made of glass and the channel bed was PVC. This channel was previously used by Chanson (2006,2007).

The water discharge was measured with a Venturi meter located in the supply line and which was calibrated on-site with a large V-notch weir. The discharge measurement was accurate within ±2%. The clear-water flow depths were measured using rail mounted point gages with a 0.2 mm accuracy. The inflow conditions were controlled by a vertical gate with a semi-circular rounded shape (∅ = 0.3 m) (Fig. 1). The upstream gate aperture was fixed during all experiments (d_1 = 0.018 m).

The air-water flow properties were measured with a double-tip conductivity probe (Fig. 2). The probe was equipped with two identical sensors with an inner diameter of 0.25 mm. The distance between probe tips was Δx = 7.0 mm. The probe was manufactured at the University of Queensland. It was previously used in several studies, including Chanson and Carosi (2007). The conductivity probe is a phase-detection intrusive probe designed to pierce the bubbles. Its principle is based on the difference in electrical resistance between air and water (Crowe at al. 1998, Chanson 2002). The dual-tip probe was excited by an electronic system (Ref. UQ82.518) designed with a response time of less than 10 μs. During the experiments, each probe sensor was sampled at 20 kHz for 45 s Depending upon the Froude number, three to four vertical profiles were recorded at different cross-sections downstream of the jump toe. Each vertical profile contained at least 30 points. The displacement and the position of the probe in the vertical direction were controlled by a fine adjustment system connected to a Mitutoyo™ digimatic scale unit with a vertical accuracy Δy of less than 0.1 mm.

Fig. 2 - Air entrainment in hydraulic jump - Fr_1 = 8.3, x_1 = 0.75 m, d_1 = 0.018 m, shutter speed: 1/80 s, flow from right to left

The analysis of the probe voltage output was based upon a single threshold technique, with a threshold set between 45% and 55% of the air–water voltage range. Below this threshold, the

probe was in air whereas it was in water for larger voltage output voltages. The single-threshold technique is a robust method that is well-suited to free-surface flows (Toombes 2002, Chanson and Carosi 2007b). The error on the void fraction was expected to be less than 1% using this technique.

For each experiment, the foot of the jump, or jump toe, was always fixed at x_1 = 0.75 m and the upstream flow depth was d_1 = 0.018 m. Based on previous experiments made with the same experimental facility, the inflow was characterised by a partially-developed boundary layer. Further details on the experimental setup and results were reported in Murzyn and Chanson (2007).

EXPERIMENTAL RESULTS

The hydraulic jump flow was a sudden transition from rapid to fluvial flow motion characterised by the development of large-scale turbulence, surface waves and air entrainment. Air bubbles were entrained at the jump toe into a free shear layer characterised by intensive turbulence production (Fig. 1 & 2). The entrained air packets were broken up in very small air bubbles as they were advected in the developing shear region. Once the bubbles were convected into regions of lesser shear, bubble collisions and coalescence led to larger air entities (bubbles, pockets) that were driven by buoyancy upwards to the free-surface. In the recirculation region above the mixing layer, strong unsteady flow reversals occurred. During the present study, the location of the jump toe was consistently fluctuating around its mean position within a 0.2 to 0.4 m range depending upon the flow conditions. The jump toe pulsations were believed to be caused by the growth, advection and pairing of large scale vortices in the developing shear layer. Pulsation frequencies F_{toe} of the jump toe were typically about 0.5 to 1 Hz. The data were close to the observations of Long et al. (1991), Mossa and Tolve (1998) and Chanson (2007) in terms of Strouhal number $F_{toe}d_1/V_1$.

Vertical profiles of void fraction C and bubble count rate F were measured at different longitudinal positions $4.1 < (x-x_1)/d_1 < 34$. Figures 3 and 4 present some typical results, where the present data are compared with the earlier data of Chanson (2006). In the developing shear layer, the data compared favourably with an analytical solution of the advective diffusion equation for air bubbles (Chanson 1997) :

$$C = C_{max} \exp\left(- \frac{((y - y_{Cmax})/d_1)^2}{4\, D^* (x - x_1)/d_1} \right) \quad (5)$$

where C_{max} is the maximum void fraction in the shear layer, y_{Cmax} is the vertical elevation of the maximum void fraction C_{max}, D^* is a dimensionless turbulent diffusivity: $D^* = D_t/(V_1 d_1)$, D_t is the air bubble turbulent diffusivity. Equation (5) is compared with some data in Figures 3A and 4A. The peak of void fraction C_{max} was clearly marked for all investigated conditions (Table 1). At a given position downstream of the toe, C_{max} increased with increasing Froude number, while, for a given Froude number, it decreased with the distance from the jump toe.

Figures 3B and 4B present some typical vertical distributions of dimensionless bubble count rate $F\, d_1/V_1$. The bubble count rate F is defined the number of air bubbles detected by the probe leading sensor per unit time and it is proportional to the specific air-water interface area. All the data exhibited a major peak of bubble count rate F_{max} in the developing shear region. It is suggested that this peak was linked with high levels of turbulent shear stresses that break up the entrained air bubbles into finer air entities. The maximum bubble count rate F_{max} increased with increasing Froude number. For Fr = 5.1, F_{max} reached 55 Hz whereas it was nearly 124 Hz for Fr = 8.3. For a given Froude number, F_{max} decreased with an increasing distance from the impingement point.

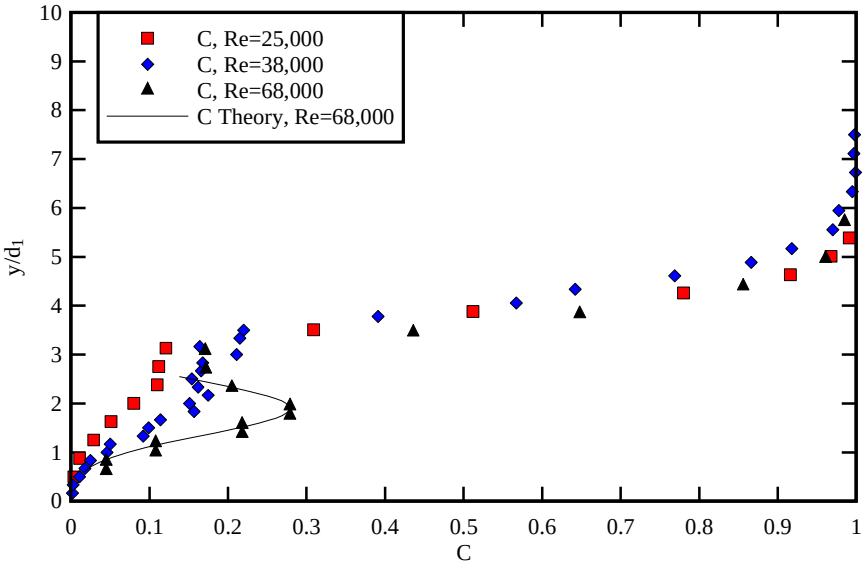

(A) Dimensionless distributions of void fraction - Comparison with Equation (5)

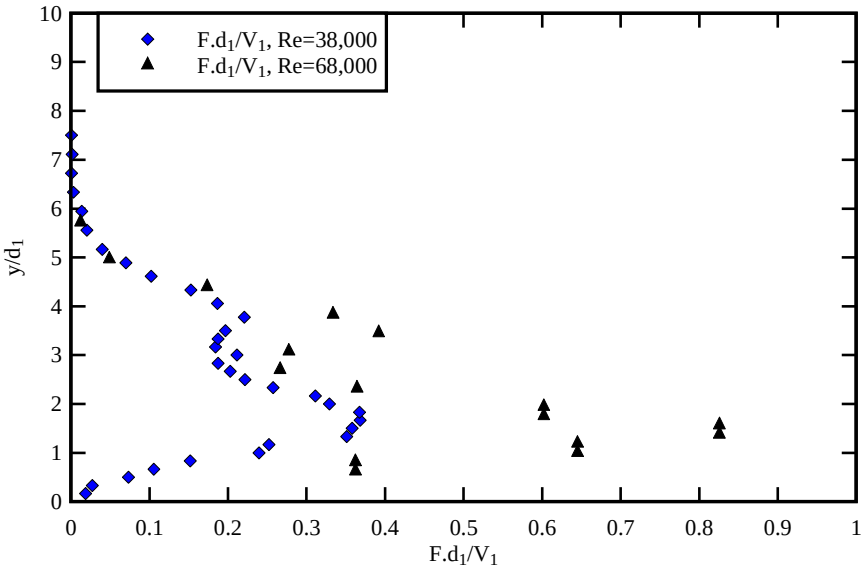

(B) Dimensionless distributions of bubble count rate $F\,d_1/V_1$

Fig. 3 - Dimensionless distributions of void fraction and bubble count rate in hydraulic jumps for $Fr_1 = 5.1$, $x_1/d_1 = 42$, $W/d_1 \geq 20$ and $(x-x_1)/d_1 = 8$, Re = 25,000, 38,000 & 68,000 - Data: Chanson (2006) and Present study (Re = 38,000)

DYNAMIC SIMILARITY IN AIR-WATER FLOW PROPERTIES

The present experiments were designed to be geometrically similar to the earlier data sets of Chanson (2006) based upon a Froude similitude with undistorted scale (Table 1). Similar experiments were conducted for identical Froude numbers Fr_1 with identical upstream distance x_1/d_1 between gate and jump toe. The air-water flow measurements were performed in the developing air-water flow region at identical cross-sections $(x-x_1)/d_1 < 34$. Typical comparative results are presented in Figures 3 and 4. The data showed drastic scale effects in

the smaller hydraulic jumps in terms of void fraction and bubble count rate distributions. The results highlighted consistently a more rapid de-aeration of the jump roller with decreasing Reynolds number for a given inflow Froude number, an absence of self-similarity of the void fraction profiles in the developing shear layer for Re < 40,000 and Fr_1 = 5.1 (Fig. 3A), and an increasing dimensionless bubble count rate with increasing Reynolds number for a given inflow Froude number (Fig. 3B and 4B).

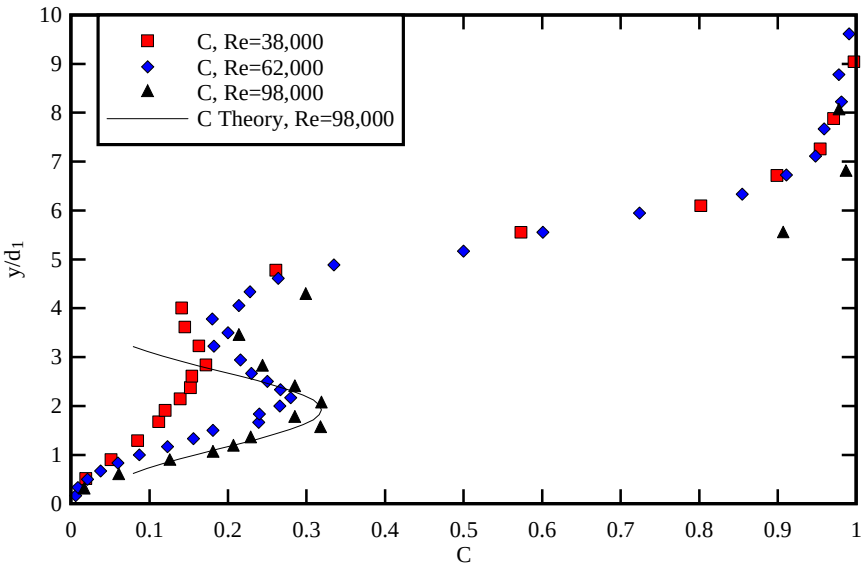

(A) Dimensionless distributions of void fraction - Comparison with Equation (5)

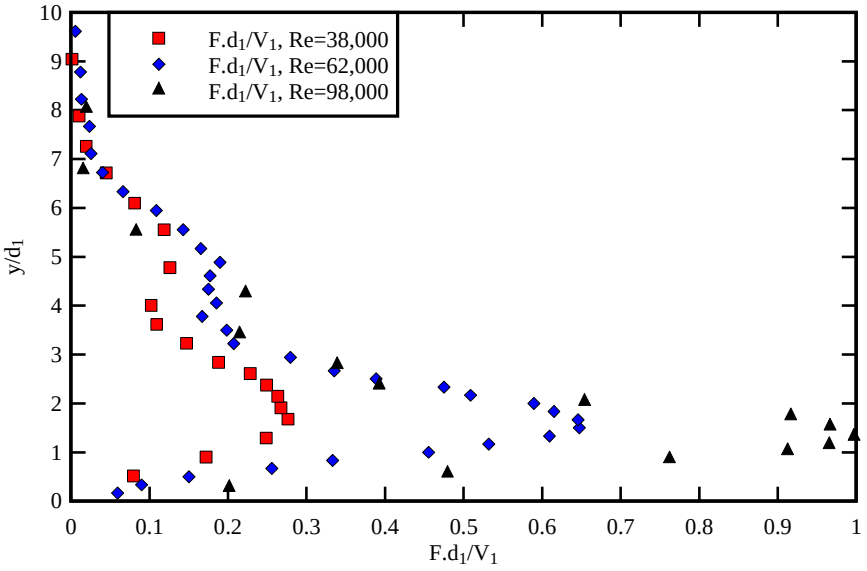

(B) Dimensionless distributions of bubble count rate F d_1/V_1

Fig. 4 - Dimensionless distributions of void fraction and bubble count rate in hydraulic jumps for Fr_1 = 8.5, x_1/d_1 = 42, $W/d_1 \geq 20$ and $(x-x_1)/d_1$ = 12, Re = 38,000, 62,000 & 98,000 - Data: Chanson (2006) and Present study (Re = 62,000)

The effects of the Reynolds number on the two-phase flow properties were particularly marked in the developed shear layer. This is illustrated in Figure 5 showing the maximum void fraction C_{max} and maximum dimensionless bubble count rate $F_{max}d_1/V_1$ in the shear layer as functions of the inflow Reynolds number Re. Figure 5A presents the relationship between C_{max} and Re, and Figure 5B shows the variation of $F_{max}d_1/V_1$ with Re. The results highlighted some monotonic increase in maximum void fraction and maximum dimensionless bubble count rate in the mixing layer with increasing Reynolds number. The rate of increase was about the same for both inflow Froude numbers Fr = 5.1 and 8.5.. Further no asymptotic limit was observed within the range of the experiments (Table 1). The relationships in maximum void fraction and bubble count, and Reynolds number were correlated by:

$$C_{max} = \frac{0.745\ Re}{Re + 1.20\ 10^5} \qquad 2\ 10^4 < Re < 10^5 \quad (6)$$

$$\frac{F_{max}\ d_1}{V_1} = 0.73 \times Ln(Re) - 7.38 \qquad 2\ 10^4 < Re < 10^5 \quad (7)$$

with a normalised coefficient of correlation of 0.978 and 0.984 respectively.

The comparative analysis highlighted that the experimental data sets with inflow Reynolds numbers up to 98,000 cannot be extrapolated to large-size prototype structures without significant scale effects in terms of void fraction and bubble count rate distributions. This result has important implications in terms of civil, environmental and sanitary engineering design. In hydraulic structures, storm water systems and water treatment facilities, hydraulics jumps operate typically with inflow Reynolds numbers ranging from 10^6 to over 10^8.

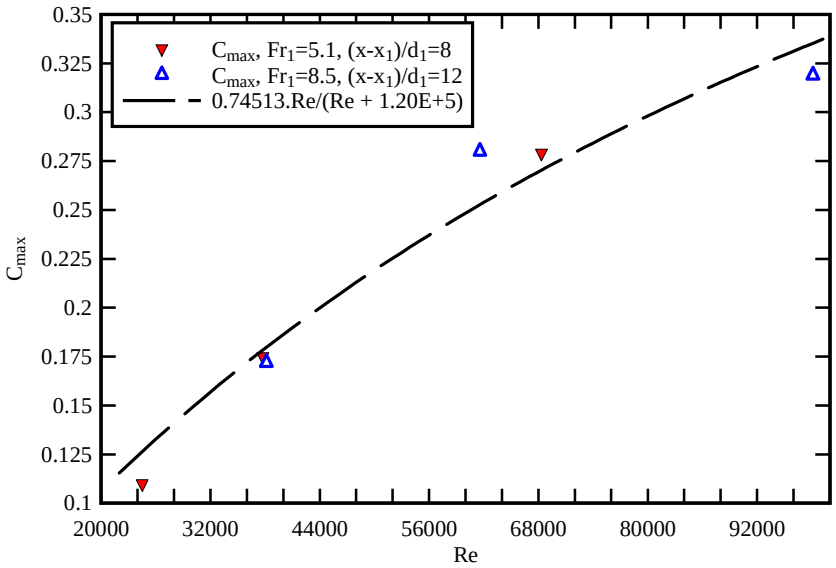

(A) Maximum void fraction C_{max} - Comparison with Equation (6)

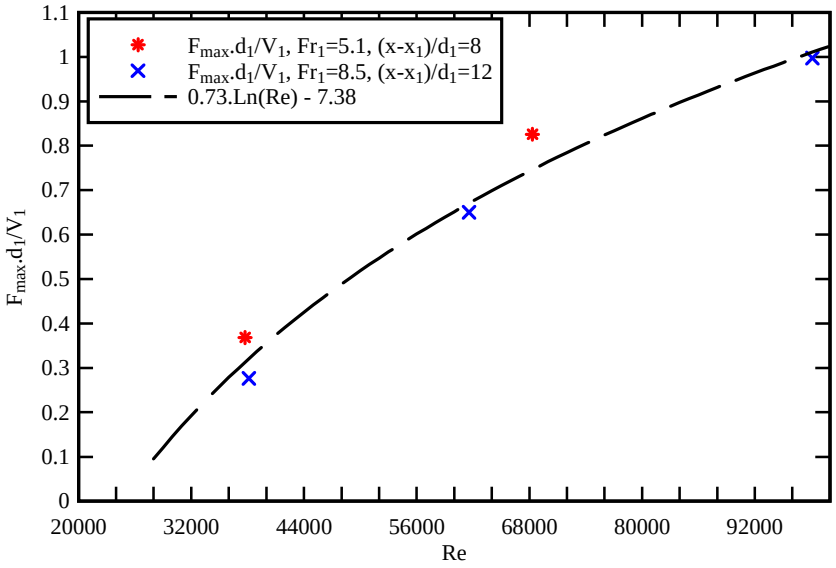

(B) Maximum bubble count rate $F_{max}d_1/V_1$ - Comparison with Equation (7)

Fig. 5 - Effects of the inflow Reynolds number on the maximum void fraction C_{max} and maximum dimensionless bubble count rate $F_{max}d_1/V_1$ in the developing shear layer - Data: Chanson (2006) and Present study

CONCLUSION

Detailed air-water flow measurements were conducted in hydraulic jumps with partially-developed inflow conditions. The void fraction distributions showed the presence of an advective shear layer in which the air concentration distributions followed an analytical solution of the diffusion equation, while the bubble count rate distributions exhibited a marked maximum in the mixing layer. Similar experiments were conducted with identical inflow Froude numbers Fr_1 and Reynolds numbers between 24,000 and 98,000 (Table 1). The results of Froude-similar experiments showed some drastic scale effects in the smaller hydraulic jumps in terms of void fraction and bubble count rate distributions. Void fraction distributions implied comparatively greater detrainment at low Reynolds numbers yielding to lesser overall aeration of the jump roller. The dimensionless bubble count rates were significantly lower in the smaller channel, especially in the mixing layer.

In a physical model, the flow conditions are said to be similar to those in the prototype if the model displays similarity of form, similarity of motion and similarity of forces. Equation (1) highlighted that the study of air bubble entrainment in hydraulic jumps required a large number of relevant parameters. The present comparative analysis demonstrated quantitatively that dynamic similarity of two-phase flows in hydraulic jumps cannot be achieved with a Froude similitude unless working at full-scale (1:1). In experimental facilities with Reynolds numbers up to 10^5, some viscous scale effects were observed in terms of the rate of entrained air, air-water interfacial area and bubble size populations.

REFERENCES

Bélanger, J.B. (1828). "Essai sur la Solution Numérique de quelques Problèmes Relatifs au Mouvement Permanent des Eaux Courantes." *Carilian-Goeury*, Paris, France (in French).

Chanson, H. (1995). "Air Entrainment in Two-Dimensional Turbulent Shear Flows with Partially Developed Inflow Conditions." ***International Journal of Multiphase Flow***, Vol.

21, No. 6, pp. 1107-1121.
Chanson, H. (1997). "Air Bubble Entrainment in Free-Surface Turbulent Shear Flows." *Academic Press*, London, UK, 401 pages.
Chanson, H. (2002). "Air-Water Flow Measurements with Intrusive Phase-Detection Probes. Can we Improve their Interpretation ?" *Journal of Hydraulic Engineering*, Trans. ASCE, Vol. 128, No. 3, pp. 252-255
Chanson, H. (2006). "Air Bubble Entrainment in Hydraulic Jumps. Similitude and Scale Effects." *Report No. CH57/05*, Dept. of Civil Engineering, The University of Queensland, Brisbane, Australia, Jan., 119 pages.
Chanson, H. (2007). "Bubbly Flow Structure in Hydraulic Jump." *European Journal of Mechanics B/Fluids*, Vol. 26, No. 3, pp. 367-384.
Chanson, H. (2007b). "Dynamic Similarity and Scale Effects Affecting Air Bubble Entrainment in Hydraulic Jumps." *Proc. 6th International Conference on Multiphase Flow ICMF 2007*, Leipzig, Germany, July 9-13, M. Sommerfield Editor, Session 7, Paper S7_Mon_B_S7_Mon_B_3, 11 pages (CD-ROM).
Chanson, H., and Brattberg, T. (2000). "Experimental Study of the Air-Water Shear Flow in a Hydraulic Jump." *International Journal of Multiphase Flow*, Vol. 26, No. 4, pp. 583-607.
Chanson, H., and Carosi, G. (2007). "Turbulent Time and Length Scale Measurements in High-Velocity Open Channel Flows." *Experiments in Fluids*, Vol. 42, No. 3, pp. 385-401 (DOI 10.1007/s00348-006-0246-2).
Chanson, H., and Carosi, G. (2007b). "Advanced Post-Processing and Correlation Analyses in High-Velocity Air-Water Flows." *Environmental Fluid Mechanics*, Vol. 7, No. 6, pp. 495-508 (DOI 10.1007/s10652-007-9038-3).
Crowe, C., Sommerfield, M., and Tsuji, Y. (1998). "Multiphase Flows with Droplets and Particles." *CRC Press*, Boca Raton, USA, 471 pages.
Henderson, F.M. (1966). "Open Channel Flow." *MacMillan Company*, New York, USA.
Long, D., Rajaratnam, N., Steffler, P.M., and Smy, P.R. (1991). "Structure of Flow in Hydraulic Jumps." *Jl of Hyd. Research*, IAHR, Vol. 29, No. 2, pp. 207-218.
Mossa, M., Tolve, U. (1998). "Flow Visualization in Bubbly Two Phase Hydraulic Jumps." *Journal of Fluids Engineering*, Trans. ASME, Vol. 120, ppP 160-165.
Murzyn, F., and Chanson, H. (2007). "Free Surface, Bubbly Flow and Turbulence Measurements in Hydraulic Jumps." *Report No. CH63/07*, Div. of Civil Engineering, The University of Queensland, Brisbane, Australia, July, 116 pages.
Murzyn, F., Mouazé, D., and Chaplin, J.R. (2005). "Optical Fibre Probe Measurements of Bubbly Flow in Hydraulic Jumps." *International Journal of Multiphase Flow*, Vol. 31, No. 1, pp. 141-154.
Murzyn, F., Mouazé, D., and Chaplin, J.R. (2007). "Air-Water Interface Dynamic and Free Surface Features in Hydraulic Jumps." *Journal of Hydraulic Research*, IAHR, Vol. 45, No. 5, pp. 679-685.
Rajaratnam, N. (1962). "An Experimental Study of Air Entrainment Characteristics of the Hydraulic Jump." *Journal of Instn. Eng. India*, Vol. 42, No. 7, March, pp. 247-273.
Resch, F.J., and Leutheusser, H.J. (1972). "Le Ressaut Hydraulique : mesure de Turbulence dans la Région Diphasique. " *La Houille Blanche*, No. 4, pp. 279-293 (in French).
Toombes, L. (2002). "Experimental Study of Air-Water Flow Properties on Low-Gradient Stepped Cascades." *Ph.D. thesis*, Dept. of Civil Engineering, The University of Queensland, Brisbane, Australia.
Wood, I.R. (1991). "Air Entrainment in Free-Surface Flows." *IAHR Hydraulic Structures Design Manual No. 4*, Hydraulic Design Considerations, Balkema Publ., Rotterdam, The Netherlands, 149 pages.